

# PERFORMANCE VERIFICATION OF THE HEAD/EYE INTEGRATED TRACKER

Jeong-ho Kim, Dae-woo Lee

*Aerospace Department, Pusan National University, Jang-jeon Dong, Pusan City, Korea*

Se-jong Heo, Chan-gook Park

*Department of Mechanical and Aerospace Engineering, Seoul National University, Seoul City, Korea*

Kwang-yul Baek, Hyo-choong Bang

*Department of Aerospace Engineering, KAIST, Daejeon City, Korea*

Keywords: Head-tracker, Eye-tracker, Integration, Sensor fusion, Dichroic filter.

Abstract: This paper describes the development of an integrated head/eye tracker system. To obtain the position and attitude of a head, the sensor-fusion head tracker is used. The head tracker combines the result of the vision-based tracking and the IMU to increase the tracking accuracy. Five sets of IR LEDs are installed on the surface of a helmet, and the IMU is installed inside the helmet; each set of LEDs comprises three LEDs positioned at the vertices of a triangle. IR LEDs are used on the eye-tracker system since they are more suitable than visible LEDs for cognizing the pupil. For the precise tracking of the pupil, three methods—intensity-based detection method, shape-based detection method, and sequential mean-shift method—are used. The gaze vector is calculated by using the obtained position of the pupil, focal length, and gaze-point equation. Finally, we verify whether this integrated system can be used in practical military equipment.

## 1 INTRODUCTION

In this study, the position and attitude of the head are measured using an IMU (inertial measurement unit), which has a high sampling rate, and a vision-based head tracking method, which guarantees a bounded error. The experiment is performed on a rate table and the results of a sensor-fusion algorithm show that the performance of the integrated system is better than that of a vision-based tracking system.

In the eye-tracking process, we track the position of the a pupil using IR(Infrared) LEDs(light-emitting diodes) and a dichroic filter, which help us obtain a clear image of the pupil. After obtaining the position of the pupil, the gaze vector can be determined using the focal length of the camera and the relationship between the measured position of the pupil and the position of the target in the scene image plane.

When the head tracker and the eye tracker are not synchronized with each other, the difference between the measured times may lead to an erroneous result. Therefore, we use a triggering signal to prevent such an error. If each system has a single thread, following the sequence is not a problem. However, if the system has many threads, one of the threads may not follow the sequence. In other words, the system may send a wrong result to the MCU and tracking will not be accurate. This paper represents a system set up in a multithreaded environment. This system can control the operation sequence of the threads by using the thread synchronization function. Finally, we evaluate the appropriateness of the thread synchronization function by considering the operation sequence of the threads, time delay for context switching, and the performance of the integrated head/eye tracker system.

This paper is subjected into three parts, head-tracker system, eye-tracker system, integrated

system and each part shows the system and the experimental results.

## 2 HEAD-TRACKER SYSTEM

### 2.1 Configuration of the Head-tracker

The system consists of IR LEDs as optical targets and an IMU fixed on the helmet; in addition, there is a stereo camera and a PC equipped with a frame grabber. Five sets of IR LEDs, with each set comprising three LEDs arranged in a triangular fashion, are fixed on the surface of the helmet.

It is necessary to carry out research to determine the pattern with the minimum number of LEDs for use in real-time tracking. In this research, five triangular patterns, which involve a lesser number of LEDs than hexagonal patterns, are used. The position and attitude are tracked well despite the number of LEDs being only three.



Figure 1: Triangular LED patterns.

### 2.2 Image Processing Algorithm

The image processing algorithm used in the hybrid head-tracker system performs feature segmentation, projective reconstruction, and model indexing. Feature segmentation extracts feature points that represent the LEDs in the image of each camera. To obtain the feature points of the LEDs, the obtained images are sequentially processed with dilation and binarization techniques for denoising. Finally, the ROI (Region Of Interest) is extracted from the image to reduce the computation time, and then ROI is treated by masking method.

In projective reconstruction, we calculate the 3D positions of feature points in the camera coordinate system of the left camera. We establish stereo correspondence using the epipolar geometry and the MHD (modified Hausdorff distance). First, the epipolar constraint is applied to find the candidate points. This constraint is expressed as  $q^T F p = 0$ , where  $F$  denotes a fundamental matrix and  $p$  and  $q$  are homogeneous expression of the position of each feature point in the image plane.  $F$  can be obtained

by camera calibration. The MHD is used to select the best point among candidate points for stereo matching. The candidate point with the minimum MHD is considered the best point for stereo matching.



Figure 2: Stereo matching.

In model indexing, the point set obtained in projective reconstruction is matched with a point in the database using triangle-pattern-based GH (geometric hashing) and the MHD (Sejong Heo).

The attitude and position of the helmet are estimated by solving the absolute orientation problem. In this study, the two coordinate systems are the helmet coordinate system and camera coordinate system.

### 2.3 Estimation of the Position and Attitude of a Helmet using a Sensor Fusion Algorithm

In this section, we introduce the fusion system, which can track the pose, position, and attitude of the helmet in the world coordinate system by using the stereo cameras and IMU installed on the helmet. The indirect method to combine the inertial and vision data is used and motion and structure estimation are performed simultaneously. This implies that no “main” sensor or “aiding” sensor is used. “Motion” refers to the position, velocity, acceleration, angular velocity, and attitude of the helmet, while “structure” refers to the 3D positions of the feature points (LEDs). Figure 3 shows the sensor fusion algorithm.

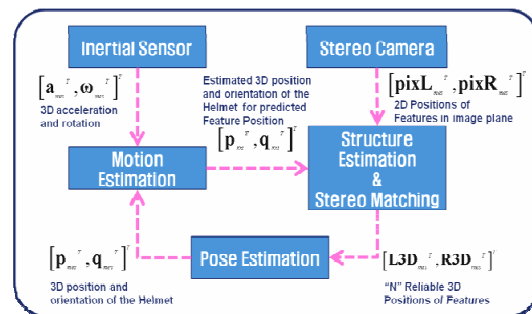


Figure 3: Flowchart of the sensor fusion algorithm.

We use the EKF for motion estimation because we use non-linear system models—non-linear measurement model of an inertial system and linear measurement model of a vision system. A block diagram of the motion estimation filter is shown in Fig. 4. (Sejong Heo).

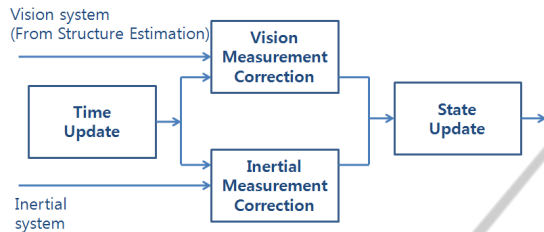


Figure 4: Block diagram of the motion estimation filter.

The structure estimation is performed by using a bank of simple EKFs. Even though new features appear on or some features disappear from the scene, the structure estimation algorithm can track the features robustly. In Fig. 5, the green lines connected to boxes with the numerals 1, 2, and 3 are the axes of the helmet coordinate system.

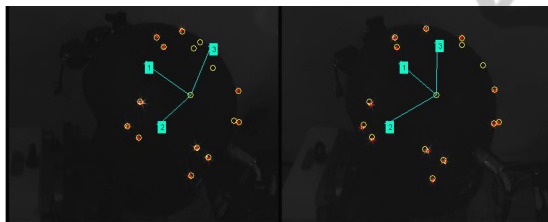


Figure 5: Feature point tracking in the structure estimation process.

### 3 EYE-TRACKER SYSTEM

#### 3.1 Configuration of the Eye-tracker

The eye-tracker system is configured by using two IR module cameras, dichroic filters, one scene camera, and a PC equipped with a frame grabber. The dichroic filters reflect infrared radiation and allow visible radiation to pass through. Thus, infrared radiation from IR LEDs is reflected to the eyes and the scene is reflected to the cameras. Thus, a user can see the front view by using these filters, without any problem.

#### 3.2 Pupil-tracking Method

In the process of the tracking the pupil, the EKF (extended Kalman filter) is used. The EKF estimates

and measures the position of the pupil and then operates only in a small region near the estimated position. Thus, this process is advantageous for reducing the computational load without decreasing accuracy. The circle fitting algorithm and sequential mean-shift are also used with the EKF.

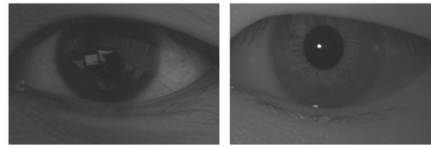


Figure 6: Clarity of eye when (left) visible radiation and (right) infrared radiation are used.

#### 3.2.1 Intensity-based Binarization

An image of the pupil is binarized by thresholding and then processed with a morphological filter to decrease the noise. In the processed image, groups of pixels are labelled, and the size, aspect ratio, and compactness of the labelled object are measured.

#### 3.2.2 Circle-detection based Tracking

The edges of the pupil image are determined by the Canny edge method. After detecting the edge, we search for the circular object by using the Hough transform method. The Canny method is more accurate than the Sobel and Laplace methods because it eliminates the small boundary by measuring the boundary. Circle detection is conducted using the Hough circle transform with predefined radius ranges.

#### 3.2.3 Sequential Mean-shift

The sequential mean-shift algorithm repeatedly performs several mean-shift operations, with the search region being progressively decreased in every successive operation. First, a wide region of the image is searched. The search region is decreased in every subsequent operation to searching more accurately. This method is robust against noise like the eyebrow and eyelid, as shown in right of Fig. 7



Figure 7 Binarized image of the pupil (left); Edge and circle detection (middle); Sequential Mean-shift (right).

### 3.3 Experimental Results

We performed experiments using the eye tracker in real-time environments. In these experiments, the user gazed at nine points for 30 s. Figure 8 shows the pupil positions measured by the above-mentioned pupil-tracking methods and the estimated positions obtained by using the Kalman filter. The upper panel gives the X-axis positions of the pupil in the image plane, and the lower panel gives the Y-axis positions. The user's blinks can cause pupil tracking to fail, as shown at 200 in Fig 8. Even if the measured position is bounced because of tracking failure, the estimated position is rapidly stabilized. The eye-tracker system shows an error within 2 pixels from the centre of a target for free head motion. We can verify that the experimenter's gaze points to the target fairly accurately.

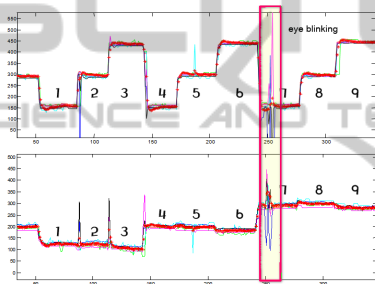


Figure 8: Tracking result for the position of the pupil: (above) x-axis and (below) y-axis.

## 4 INTEGRATED TRACKING SYSTEM DEVELOPMENT

### 4.1 Experimental Results

The integrated system is configured by using a head-tracker system, eye-tracker system, and Main Control Unit (MCU) as shown in Fig. 9.

In this integrated system, synchronization between the head tracker and eye tracker is very important for high accuracy. If the two systems are not synchronized with each other, then each system obtains the image of the helmet or pupil at different times and this may lead to an error when a target is moving fast.

This paper presents a synchronization method that involves the use of a trigger signal from the MCU. Using this method, we can synchronize the head-tracker system and eye-tracker system and integrate the tracking results from both systems onto an integrated coordinate. The MCU also provides all information on a monitor.

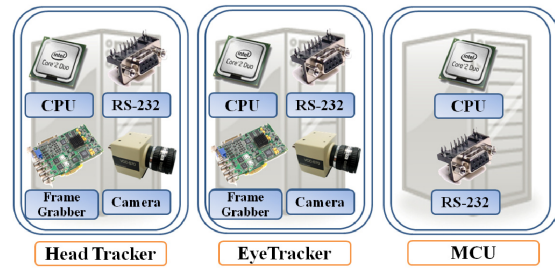


Figure 9: Configuration of the integrated system.

The gaze-tracking system has to consider the relationship between the head and eye. Without this consideration, gaze tracking that is performed by making assumptions such as the head or gaze direction being fixed

### 4.2 Experimental Results

The experimental equipment consists of the head/eye-tracker system and a beam projector, as shown in Fig. 10.

Because it is difficult to determine the centre of the projector, we define the location of the image centre as a coordinate origin. It is also necessary to calibrate the error between an image centre and the coordinate origin of the head/eye-tracker.

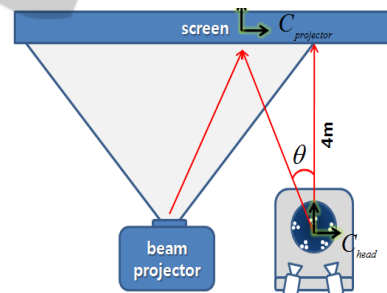


Figure 10: Schematic of the experiment.

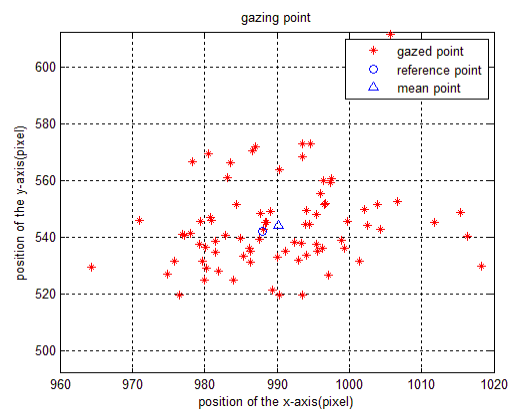


Figure 11: Gazing points on the screen.

**4.2.1 Case of One-point Gazing with the Attitude of the Head Fixed**

Figure 11 shows results for the case of one-point gazing when the attitude of the user’s head is fixed. The circle indicates the reference (target) point, and the stars. The errors between the reference point and the mean value when the user gazes 4 m ahead are  $(x, y) = (0.45 \text{ cm}, 0.37\text{cm})$  and the standard deviation is  $(2.07 \text{ cm}, 3.06 \text{ cm})$ .

Figure 12 presents the time histories of yaw and pitch for the head tracker, eye tracker, and integrated head/eye tracker systems. There are irregular jumps on the graph for the head tracker compared to the eye tracker. These jumps occur simultaneously in the yawing and pitching movements. The reason for the jumps is the increase or decrease in the number of LED sets.

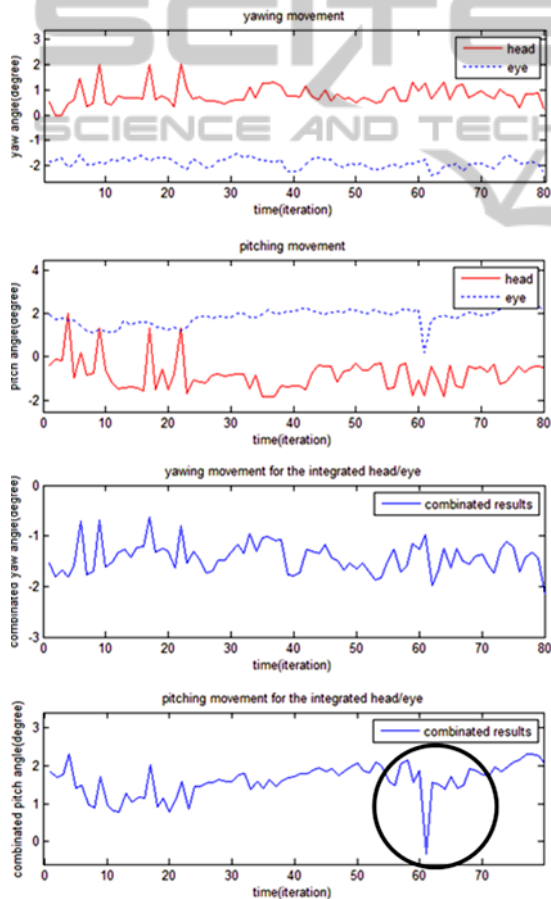


Figure 12: Results of the experiment.

The circled part on the graph of pitching movement for the integrated head/eye integrated system (fourth graph) dilates on twinkle, which affects the tracking performance. Besides twinkle, there are several error factors like difficulty in

maintaining a constant attitude of the head with the helmet and difficulty in continuously gazing at one point, etc.

**4.2.2 Case of One-point Gazing with Varying Attitude of the Head**

All notations in Fig. 13 are the same as those of Fig. 13. The error between the reference point and mean value when the user gazes 4 m ahead are  $(x, y) = (0.45 \text{ cm}, 0.325 \text{ cm})$  and the standard deviation is  $(5.45 \text{ cm}, 5.06\text{cm})$ .

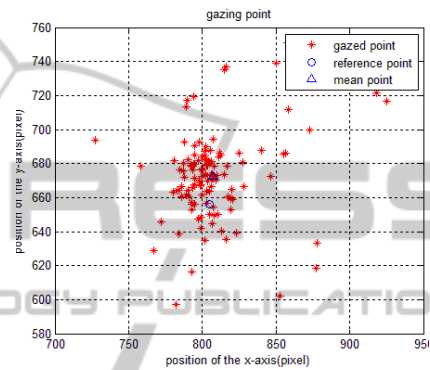


Figure 13: Gazing point on the screen.

In this section, we performed an experiment for the case of one-point gazing with a varying attitude of the head. The first graph in Fig. 14 shows that initially, the head is shifted toward the left side by  $9^\circ$  and the eyes gaze at the centre of the screen. After 32 iterations, the head is turned left by  $20^\circ$ . Finally, the head is turned right by  $8^\circ$  and the eyeballs move left by  $10^\circ$ , as shown in the circle in the first graph of Fig. 14

A positive yaw angle implies right rotation and a negative yaw angle indicates left rotation. Although the directions of the head and gaze are opposite, eyes become gaze at reference point. From these results, we can verify irregular time histories for eyes because the user’s eyes are turned away from the gazing point whenever the head is turned.

Although we try to reduce the pitch movement, we cannot prevent it because of the structural characteristics of the neck and head. These errors are observed as short-period sudden variations and are unavoidable.

The other factors responsible for short-period sudden variations are blinks and an increase or decrease in the number of LED sets in the head-tracker system, similar to the preceding case. The errors resulting from an increase or decrease in the number of LED sets are within  $3^\circ$ .

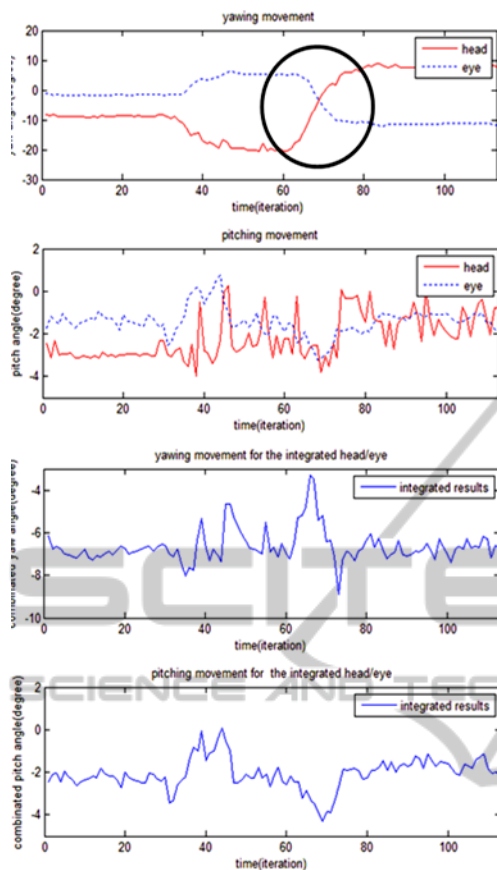


Figure 14: Results of the experiment.

## 5 CONCLUSIONS

This paper discusses the development of an integrated head/eye tracker. A user can gaze at a target during free head motion. The position of the user's head and gaze direction can be determined by using head/eye-tracker system.

The head-tracker and eye-tracker systems commence operations following the triggering signal from the MCU; all processed data are stored in the MCU. The collected data are integrated and converted to integration coordinates. During the whole process, all information about tracking is presented on the screen of the MCU, and a 3-D model helps understand the state of the user.

The integrated head-tracker system developed in this study shows a 7-mm error for translation motion of 0.3 m and 0.0329deg error for the rotation of the helmet. The eye-tracker system shows an error within 2 pixels from the centre of a target for free head motion. The tracking result is indicated by the cross hair of the scene camera installed on a top of

the helmet on an image captured by it. A 3D model helps in understanding the tracking status.

As indicated by the experimental results, while there are small errors in the time histories of the yaw, there are many short-period sudden variations in the time histories of the pitch.

The integrated head/eye-tracker system can track the target continuously when the head is turning. From this fact, it is clear that this integrated head-tracker system can be used as an effective substitute input system.

## ACKNOWLEDGEMENTS

This research is supported by vision based collision avoidance project of the Korean Aerospace Research Institute(KARI) and thank you for the support.

## REFERENCES

- Fakhr-eddine Ababsa and Malik Malle, "Inertial and Vision Head Tracker Sensor Fusion Using a Particle Filter for Augmented Reality Systems", *Circuits and Systems, 2004. ISCAS '04. Proceedings of the 2004 International Symposium in Vol.3*, 23–26 May 2004, pp. 861-4.
- Sejong Heo, Okshik Shin, and Chan Gook Park, "Estimating Motion Parameters of Head by Using Hybrid Extended Kalman Filter", *ION GNSS, 2009*.
- Youngil Kim, Youngjun Lee, and Chan Gook Park, "An Optical Helmet-Tracking System Using EKF-Based PF", *AIAA Guidance, Navigation and Control Conference and Exhibit, Honolulu, Hawaii, August 18–21*.
- D. Comaniciu, V. Ramesh, and P. Meer, "Real-Time Tracking of Non-Rigid Objects Using Mean Shift", *Conference on Computer Vision and Pattern Recognition, 2000*.
- E. Foxlin, Y. Altshuler, L. Naimark, and M. Harrington, "FlightTracker: A Novel Optical/Inertial Tracker for Cockpit Enhanced Vision", *IEEE/ACM International Symposium on Mixed and Augmented Reality (ISMAR 2004), Washington, D.C., Nov. 2–5 2004*.